universe

MDPI

Article

De Sitter Holography: Fluctuations, Anomalous Symmetry, and Wormholes

Leonard Susskind [1,2]

[1] Stanford Institute for Theoretical Physics, Department of Physics, Stanford University, Stanford, CA 94301, USA; sonnysusskind@gmail.com
[2] Google, Mountain View, CA 94043, USA

Abstract: The Goheer–Kleban–Susskind no-go theorem says that the symmetry of de Sitter space is incompatible with finite entropy. The meaning and consequences of the theorem are discussed in light of recent developments in holography and gravitational path integrals. The relation between the GKS theorem, Boltzmann fluctuations, wormholes, and exponentially suppressed non-perturbative phenomena suggests that the classical symmetry between different static patches is broken and that eternal de Sitter space—if it exists at all—is an ensemble average.

Keywords: fluctuations; symmetry; wormholes

Citation: Susskind, L. De Sitter Holography: Fluctuations, Anomalous Symmetry, and Wormholes. *Universe* **2021**, *7*, 464. https://doi.org/10.3390/universe7120464

Academic Editor: David Mattingly

Received: 17 September 2021
Accepted: 4 November 2021
Published: 29 November 2021

1. Introduction

All phenomena in a region of space can be described by a set of degrees of freedom localized on the boundary of that region, with no more than one degree of freedom per Planck area.

The Holographic Principle has been the driving force behind many of the advances in quantum gravity over the last twenty-five years, but to date, the only precise examples have been cosmologies, which, like anti-de-Sitter space, have asymptotically cold[1], time-like causal boundaries. The reliance on the existence of such boundaries is troubling because the space we livedoes not seem to have them. Instead it has a horizon and a space-like warm boundary. If the HP is to apply to the real world, then we need to generalize it.

Does the Holographic Principle apply to cosmologies such as de Sitter space? If yes, then what are the rules? I do not know for sure, and this paper will not conclusively answer the question; however, I will try to lay out some tentative principles.

Two things that will not be found here are specific models and applications to phenomenology.

1.1. An Obstruction? Or Not

Goheer, Kleban, and I (GKS) [1] proved that it is impossible for a quantum system to satisfy the symmetries of classical de Sitter space if the entropy is finite[2]. At the time, I interpreted this as a no-go theorem for absolutely stable (eternal) de Sitter space, but recent developments in quantum gravity suggest that a different interpretation might be possible. The idea is that a de Sitter vacuum might be eternal but the symmetries only approximate, as they are violated by exponentially small non-perturbative effects. The mechanisms are very similar to ones that have recently been uncovered in the SYK system and its gravitational dual.

1.2. Eternal de Sitter Space

By eternal de Sitter space, I mean a cosmology that is trapped in a state of finite entropy and cannot escape through reheating or tunneling to a larger "terminal vacuum" [2–6]. Eternal de Sitter spacemight arise from a landscape in which the scalar fields have a strictly positive potential, greater than some finite positive gap, in which there is one or more minima of V. Figure 1 illustrates this kind of potential. I do not know if a landscape with

these properties can exist in a real theory of quantum gravity, but let us assume that it can, and see where this takes us.

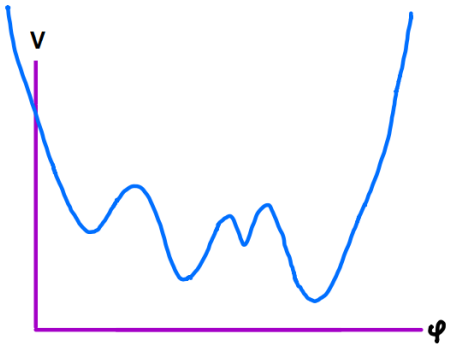

Figure 1. A schematic landscape for eternally stable de Sitter space. The universe spends most of its time in the lowest minimum with rare fluctuations to higher points.

Classically, the different minima lead to different stable de Sitter geometries, but in quantum mechanics, tunneling allows for transitions between the minima. This leads to a single thermal equilibrium state (of a static patch), which mostly sits in the lowest minimum. Howver, occasional Boltzmann fluctuations allow for transitions to higher minima, followed by tunneling back to the lowest minimum. The rates for such fluctuations are of the order $\exp(-S_0)$, where S_0 is the nominal entropy of the de Sitter space at the lowest minimium[3]. Other, less extreme fluctuations can occur; for example, the horizon of a static patch may spontaneously emit an object such as a black hole. These freak fluctuations are the only things that occur in the closed quantum world of a de Sitter static patch [7,8], but thermal correlations contain a wealth of information about non-equilibrium dynamics.

Eternal de Sitter spaceis, of course, eternal, both to the future and to the past[4]. Among the possible Boltzmann fluctuations that can occur over an enormous expanse of time are transitions to what we ordinarily think of as the initial conditions of our universe. Consider a fluctuation to to an inflationary point on the landscape, which, after some inflation, eventually evolves to a standard Λ-CDM universe. That would not be the end of the story. After a very long period of Λ-dominance, a fluctuation will occur to another minimum, and the whole process will repeat.

While this may be possible, a theory based on Boltzmann fluctuations is a very implausible framework for cosmology. In order to escape the eternal cycle of recurrences, near recurrences, partial recurrences, and freak histories described in [8], it seems necessary to have a landscape that includes terminal vacua [2,3]. A phenomenon called "fractal flow" [4–6] can then lead to a much more plausible cosmology.

Nevertheless, it is interesting to explore the consequences of the Holographic Principle for eternal de Sitter space, even if this eventually leads to the conclusion that eternal de Sitter space is inconsistent.

2. Static Patch Holography

A number of different approaches to de Sitter space might loosely be called holographic. I will stick to the original meaning of the term: a description localized on the boundary of a spatial region in terms of a quantum system without gravity. Specifically, we will focus on static patches and their boundaries—cosmic horizons. I will not speculate on the details of the quantum system other than to say that it should be fairly standard; for example, it might be described as a collection of qubits, or some form of matrix quantum mechanics with a Hermitian Hamiltonian. The bulk space–time and its geometry emerge from the holographic degrees of freedom.

2.1. The Semiclassical Limit

The classical limit of de Sitter space is described by the metric,

$$\begin{aligned} ds^2 &= -f(r)dt^2 + f(r)^{-1}dr^2 + r^2 d\Omega_2^2 \\ f(r) &= \left(1 - \frac{r^2}{R^2}\right) \end{aligned} \tag{1}$$

The length-scale R is the radius of curvature, inverse to the Hubble parameter. The cosmic horizon at $r = R$ is the place where $f(r) = 0$.

The semiclassical limit refers to the theory of small perturbations about the classical geometry, which can be described in powers of $\hbar$. Although it may be sufficient for many purposes, the semiclassical theory is incomplete. The full quantum theory will have non-perturbative effects of magnitude

$$\exp\left(-\frac{a^2}{G\hbar}\right),$$

where a is a characteristic length scale and G is Newton's constant. If $a \sim R$, then the nonperturbative effects are of the order

$$\exp\left(-S_0\right),$$

S_0, which is the de Sitter entropy. In the semiclassical limit, only the zero-order term in $\exp\left(-S_0\right)$ is retained.

De Sitter space is, in some ways, similar to a black hole. Both have horizons, an entropy proportional to the horizon area, and a temperature. Both have a semiclassical limit and additional non-perturbative effects. For any real black hole, the nonperturbative effects are exponentially small (in the entropy), but play a crucial role in establishing the consistency between quantum mechanics and gravity. It seems reasonable that the same would hold true for de Sitter space. Sections 3–5 discuss these nonperturbative effects but we will focus on the semiclassical theory.

To illustrate the static patch, consider the example of $(1+1)$-dimensional de Sitter space. The conformal diagram is a rectangle that is twice as wide as it is high, and periodically identified,[5] as illustrated in Figure 2.

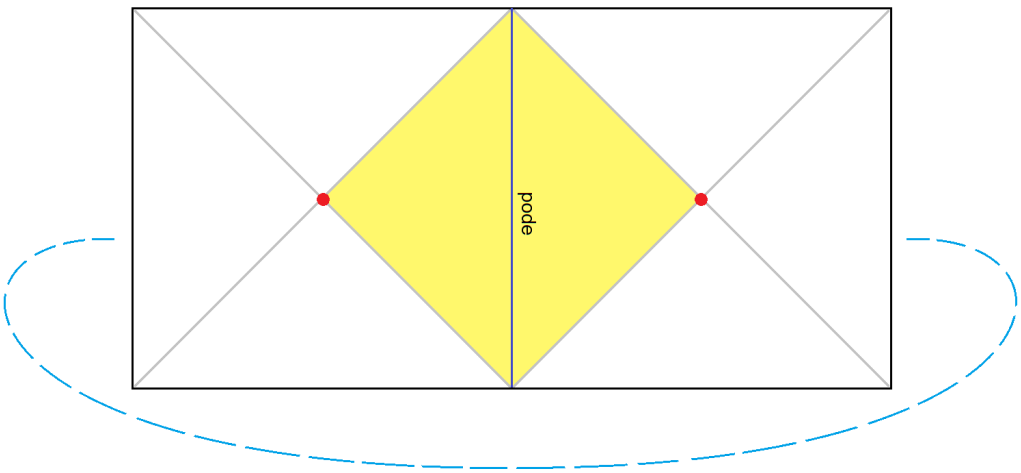

Figure 2. Conformal diagram for 2D de Sitter space and the static patch defined by a past and future pair of asymptotic points. The static patch (yellow) is the intersection of the causal future of the past point and the causal past of the future point. The intersection of the two light cones, shown as red dots, defines the bifurcate horizon. The dashed blue curve indicates identification of the left and right edges.

A static patch is defined by picking a pair of points[6], one on the asymptotic past and one on the asymptotic future. The static patch is the intersection of the causal future of the past point and the causal past of the future point. The geodesic connecting the asymptotic points will be referred to as the world-line of the "pode".

Observers who spend their entire existence in the static patch will see their world as bound by the horizon although the full geometry has no boundary. Our central hypothesis is that everything that occurs in the static patch can be described by a unitary holographic system with the degrees of freedom located at the stretched horizon (see Section 2.2). The holographic quantum mechanics, which include a Hilbert space and a Hermitian Hamiltonian, allow us to define certain thermal properties of the static patch, including a density matrix, a temperature $T = 1/\beta$, and an entropy S_0.

$$\begin{aligned} \rho &= \frac{e^{-\beta H}}{Z} \\ \beta &= \frac{1}{T} = 2\pi R \\ S_0 &= \mathrm{Tr}\,\rho \log \rho = \frac{\beta R^2}{G} \end{aligned} \tag{2}$$

In addition to the quantum mechanics of a single static patch, we also require transformation laws between static patches. For example, in Figure 3, we see two static patches of dS_2.

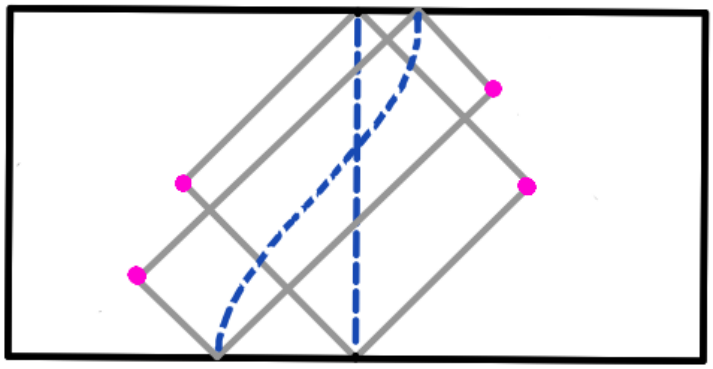

Figure 3. Two static patches in the same dS.

A theory of de Sitter spaceshould have transformation rules relating conditions in different static patches. In classical GR, these transformations are symmetries that express the identical nature of the patches. These symmetries, relating static patches and the possibility of representing them in a holographic theory, are the main subject of this paper.

The Penrose diagram for general dimensional de Sitter space is shown in the top panel of Figure 4.

The diagram shows that static patches come in matched pairs—blue and pink in the diagram. We will refer to the points at the centers of these static patches as the pode and the antipode.

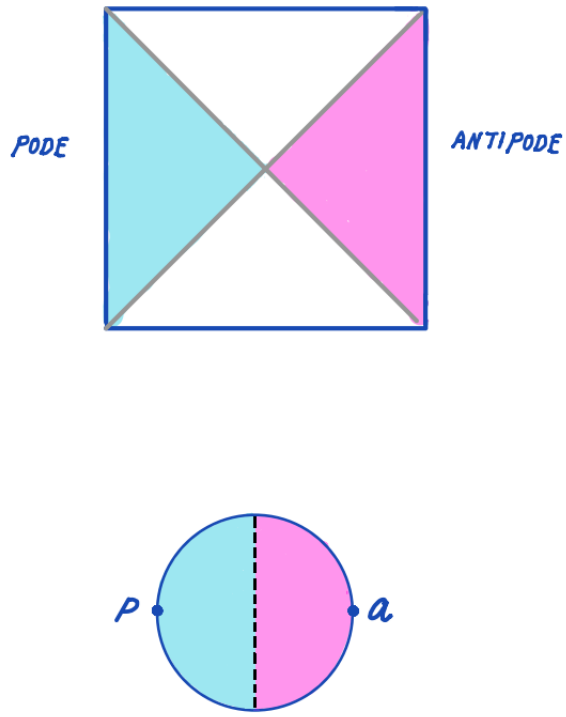

Figure 4. Upper panel: Penrose diagram for higher-dimensional de Sitter space. Static patches come in pairs and the center of these patches are referred to as the pode and the antipode. **Lower panel**: the geometry of the $t = 0$ slice of de Sitter spaceis a sphere with the pode at one pole and the antipode at the other. The dashed surface midway between the pode and antipode is the bifurcate horizon.

2.2. Where Is the Hologram?

The penrose diagram of Figure 4 looks a lot like the diagram for the two-sided AdS eternal black hole [10]. From all that we know about such black holes this suggests (and we will assume) that the podal and antipodal degrees of freedom are uncoupled, but entangled in a thermofield-double state. However the geometries of the two-sided black hole and de Sitter space are very different. In the lower panel of Figure 4, we see a time-symmetric slice through the de Sitter spacegeometry at $t = 0$. The geometry of the slice is a sphere. By contrast, the corresponding slice through the eternal black hole would be a wormhole connecting two infinite asymptotic boundaries. The spatial slice of de Sitter spacehas no boundary, with the pode and antipode being points at which the geometry is smooth.

Instead of being located at the boundary, as in AdS, the holographic degrees of freedom of the static patch is located at the (stretched) horizon. Consider Bousso's generalization [11] of the Penrose diagrams for the AdS eternal black hole, and for de Sitter space[7] These are shown in Figure 5.

Where should we locate the holographic screens (tips of the wedges) so that the maximum entropy of the spatial region described by the hologram is sufficient to encode everything in the geometry? In Figure 6 the diagrams are shown for AdS, in which we place the screens near the horizon in the first case and near the boundary in the second case.

From the light-sheet entropy bounds of [11,12], one can see that, in the first case, the maximum entropy on the pink spatial region is just a tiny bit larger than the black hole entropy. Placing holographic degrees of freedom at these locations would allow for enough degrees of freedom to describe the black hole, but not enough to describe phenomena in the bulk far from the horizon.

In the second case, where the wedges are near the boundary, the maximum entropy grows as the screens are moved outward. This is the well-known reason that the holographic degrees of freedom of AdS are located at the boundary.

Next, consider de Sitter space. In Figure 7, two choices for the locations of holographic screens are shown. In the upper panel, the screen is shown near the pode.

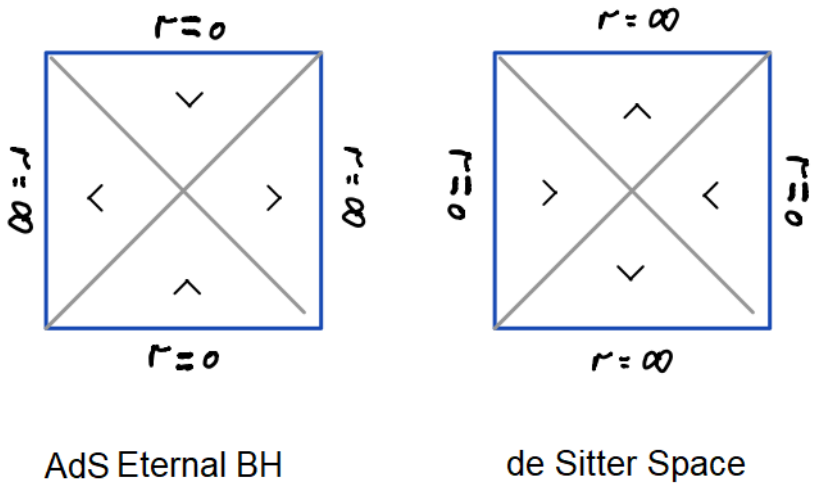

Figure 5. Penrose diagrams supplemented with Bousso wedges for the AdS eternal black hole and for de Sitter space.

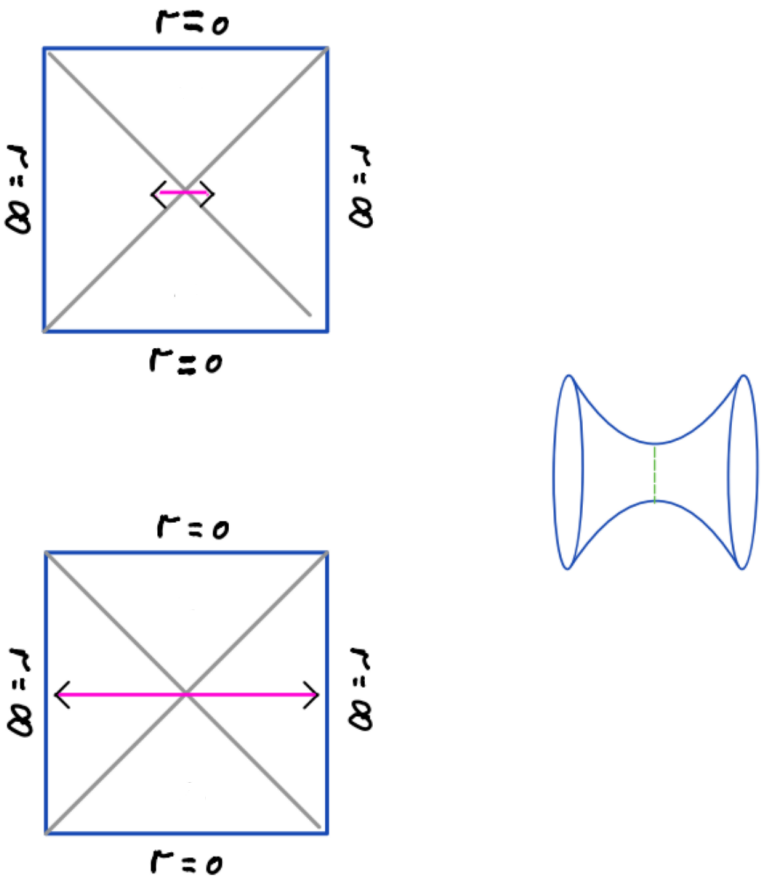

Figure 6. The AdS eternal black hole case: the upper panel introduces screens close to the horizon. According to the light-sheet entropy bound, the number of degrees of freedom on the screens is sufficient to represent the states of the black hole, but not sufficient to represent degrees of freedom in the space far from the horizons. In the lower panel, the screens are placed out near the AdS boundaries. In this case, the degrees of freedom on screens is sufficient to encode the entire space.

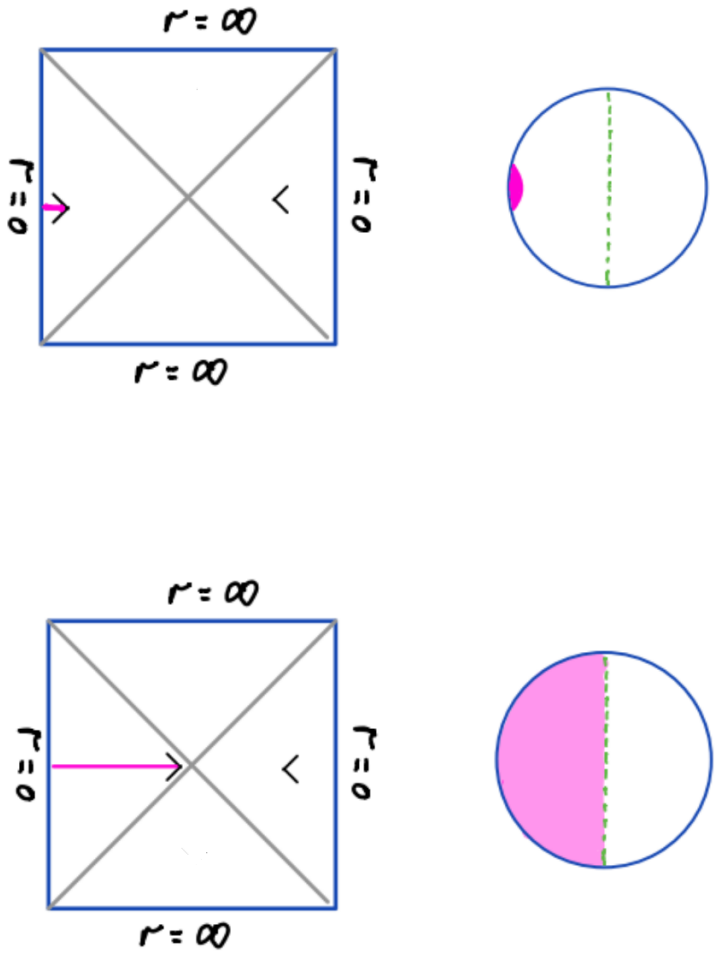

Figure 7. Penrose–Bousso diagrams for de Sitter space. In the upper panel, the screen is near the pode and the screen has almost no degrees of freedom. In the lower panel, the screen is near the horizon and the number of degrees of freedom is sufficient to encode the entire static patch.

The maximum entropy is very small when the screen is near the pode. By contrast, in the lower panel, the screen is shown close to the horizon. The maximum entropy on the pink slice, in this case, is large enough to describe the entire static patch. This is the argument for locating the holographic degrees of freedom at the horizon.

The Penrose diagram suggests that there are two sets of degrees of freedom—one for the pode and one for the antipode—located on the stretched horizons of each side, and entangled in a thermofield-double state (see Figure 8).

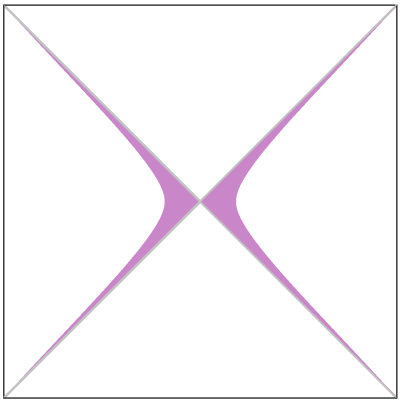

Figure 8. The stretched horizons of the pode and antipode patches.

2.3. Symmetry of de Sitter Space

Suppose that an oracle handed us what he claimed to be a holographic dual of de Sitter space. How would we know if it really describes de Sitter spaceor if it something else—perhaps a black hole? The answer is symmetry. There are many static patches in de Sitter spaceand the symmetry of the space transforms from one to another. The most conclusive test would be to show that the model satisfies the de Sitter spacesymmetry. In Figure 3, we see that one static patch can probe the region behind the horizon of another. Since the original pode-patch is described by unitary evolution, establishing that the symmetry is satisfied would tell us that all static patches are described by unitary evolution. To put it another way, testing the de Sitter symmetry also tests for the existence of space–time behind the horizon. Without testing the symmetry, there is no compelling reason to think that a given quantum system represents dS.

The symmetry of clasical d-dimensional de Sitter space is $O(d,1)$, a non-compact version of the orthogonal group $O(d+1)$. $O(d,1)$ has

$$\frac{d(d+1)}{2}$$

generators. Of these,

$$\frac{(d-2)(d-1)}{2}+1$$

generate transformations that keep the pode, antipode, and the horizon fixed. I will refer to these as the "easy" generators. They include rotations R about the pode–antipode axis and the boost-Hamiltonian H.

In addition, there are $(d-1)$ rotations $\mathcal{J}$, which rotate the positions of the pode and antipode, and other $(d-1)$ boost operators $\mathcal{K}$ that also move the pode, antipode, and horizon. These will be referred to as the "hard" generators.

As an illustration, here is the complete algebra for $d=3$,

$$\begin{aligned}
[R,H] &= 0\\
[R,\mathcal{J}] &= i\epsilon_{ij}\mathcal{J}_j\\
[R,\mathcal{K},] &= i\epsilon_{ij}\mathcal{K}_j\\
[\mathcal{J}_i,\mathcal{J}_j] &= i\epsilon_{ij}R\\
[\mathcal{K}_i,\mathcal{K}_j] &= -i\epsilon_{ij}R\\
[\mathcal{J}_i,\mathcal{K}_j] &= i\epsilon_{ij}H\\
[H,\mathcal{K}_i] &= -i\epsilon_{ij}\mathcal{J}_j\\
[H,\mathcal{J}_i] &= i\epsilon_{ij}\mathcal{K}_j
\end{aligned} \tag{3}$$

2.4. Four-Step Protocol

What follows is a schematic protocol to test the oracle's claim. If it succeeds, then the oracle's purported dual is legitimate. If it fails, then we know that he is a phony.

There is a middle ground. Suppose the protocol succeeds to some very high level of accuracy, but fails beyond this level. Then, we should check whether the small violations have a plausible gravitational explanation. As we will see, this is not just an academic possibility.

The protocol is probably consistent at the semiclassical level—in other words, to all orders in perturbation theory. Beyond that, at the level of exponentially small non-perturbative effects, the protocol must fail, but there is a plausible gravitational explanation for the failure involving a higher genus[8] saddle points in the gravitational path's integral.

To formulate the protocol, we first break the de Sitter symmetry by choosing a pair of static patches: the pode and the antipode. This is not a real symmetry-breaking; in the semiclassical theory, this is gauge-fixing[9]. If the theory is gauge-invariant, then the results of any physical calculation should not depend on the gauge, which, in this case, means the particular pair of asymptotic points used to define the static patch.

1. Step one begins with a candidate for the dual of the static patch. It consists of a conventional quantum system: a Hilbert space $\mathcal{H}_{\mathbf{p}}$ of states; a Hamiltonian $H_{\mathbf{p}}$; and a set of Hermitian observables, including the easy generators of the subgroup that hold the pode fixed. These generators include the Hamiltonian $H_{\mathbf{p}}$ and the rotation generators $R_{\mathbf{p}}$ that rotate the static patch around the pode. The easy generators are collectively denoted as $G_{\mathbf{p}}$.
   The system is assumed to be in thermal equilibrium at some definite temperature[10] T and entropy S.
2. Step two introduces another copy of the system, labeled **a** (for antipode). The doubled system has Hilbert space
$$\mathcal{H} = \mathcal{H}_{\mathbf{p}} \otimes \mathcal{H}_{\mathbf{a}}. \tag{4}$$
   The total Hamiltonian is
$$H = H_{\mathbf{p}} - H_{\mathbf{a}}. \tag{5}$$
   The Hamiltonian $H_{\mathbf{a}}$ is identical to $H_{\mathbf{b}}$. The full Hamiltonian generates a boost that translates one side of the Penrose diagram (the pode side) upward, and the other side downward.
   The full rotation generators acting on $\mathcal{H}$ are
$$R = R_{\mathbf{a}} + R_{\mathbf{b}}. \tag{6}$$
   More generally,
$$G = G_{\mathbf{a}} \pm G_{\mathbf{b}}, \tag{7}$$
   the minus sign is chosen for the Hamiltonian.
   As de Sitter spaceis spatially closed without a boundary, we must impose gauge constraints,
$$G|\Psi\rangle = 0 \tag{8}$$
   on the physical states.
   To date, none of this is unusual and it can easily be satisfied in many ways. This is why I call G the "easy" generators. Another way to characterize them is to consider them the generators that commute with the Hamiltonian. Finally, the easy generators do not couple the pode and antipode degrees of freedom.
3. The third step involves the construction of the remaining "hard" generators of $O(d,1)$, those that displace the pode and antipode. Let us call them $\mathcal{G}$. They consist of the remaining rotation generators $\mathcal{J}$ and an equal number of boosts $\mathcal{K}$. The hard generators non-trivially couple the pode and antipode degrees of freedom. Together, the easy and hard generators form the $O(d,1)$ algebra.
   This third step may not be possible. There may be no choice of $\mathcal{G}$ that satisfies the commutation relations (17). This in itself may not be fatal if the algebra can be realized to a sufficiently high degree of accuracy. For example, the violations may be exponentially small $\sim \exp(-S_0)$. The symmetry may be satisfied to a leading order in an expansion in e^{-S_0}, with the violations only occurring in higher orders. We will see in Section 5.1 that this is exactly what the GKS anomaly tells us must happen. For now, let us assume that the $\mathcal{G}$ can be constructed.
4. The final step, assuming the others have been successful, is to impose hard gauge constraints,
$$\mathcal{G}|\Psi\rangle = 0. \tag{9}$$

Note that the hard gauge constraints (9) automatically imply easy gauge constraints (8), but the reverse is not true. As in step 3, if the entropy is finite, this may only be possible for exponential precision.

If no states satisfy the gauge constraints,

$$\begin{aligned} G|\Psi\rangle &= 0 \\ \mathcal{G}|\Psi\rangle &= 0, \end{aligned} \tag{10}$$

then we stop, go back, and choose another candidate until we find one that has at least one gauge-invariant state.

The crucial gauge-invariant state is the de Sitter vacuum, which looks thermal to observers in the pode and antipode patches. This state is the thermofield-double,

$$|TFD\rangle = \sum_i e^{-\frac{\beta E_i}{2}} |E_i\rangle_{\mathbf{a}} |\bar{E}_i\rangle_{\mathbf{b}}. \tag{11}$$

which must satisfy the gauge constraints, at least to leading order, in $\exp(-S_0)$. I do not see any reason why there should be other gauge-invariant states, but this seems to be controversial. In any case, the discussion in this paper is about the state in (11).

We will return to these symmetry issues, but first I want to digress and describe a toy model, which can provide a source of intuition about de Sitter static patches.

3. Toy Model

The motivation for the toy model is the observation that the pode is a point of unstable equilibrium. Imagine a light test-particle located exactly at the pode. Consider a second test-particle located a tiny distance from the pode. Assume the second particle is initially at rest relative to the pode, and subsequently follows a geodesic. Geodesic deviation will cause that particle to fall away from the pode with the separation exponentially increasing. This is illustrated in Figure 9.

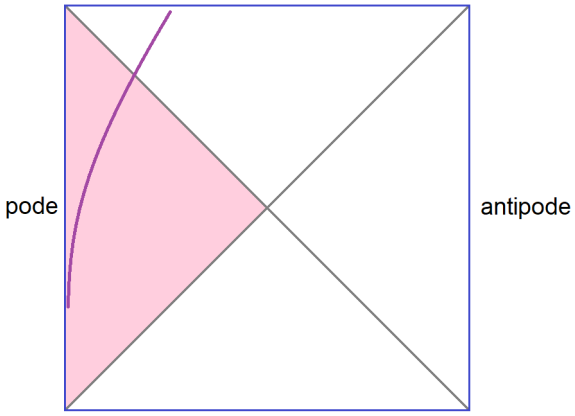

Figure 9. The pode is a point of instability. A particle arbitrarily close to the pode will depart (exponentially) from the pode, and will eventually fall through the horizon. Classically, it will take a logarithmically infinite coordinate time to reach the horizon.

To model this behavior, we can consider a non-relativistic particle in an inverted, three-dimensional, harmonic oscillator potential,

$$H = \sum_i \frac{p_i^2 - x_i^2}{2} \qquad (i = 1, 2, 3) \tag{12}$$

The unstable equilibrium point $x_i = 0$ corresponds to the pode. The spectrum of H is continuous and runs over all real numbers. The energy eigenfunctions at a large x have the form,

$$\psi \to e^{\pm ix^2/2}. \tag{13}$$

Classically, if the particle starts near the top of the potential, the subsequent motion satisfies,

$$\begin{aligned} r &\equiv \sqrt{|x|^2} \to e^t \\ |p| &\to e^t, \end{aligned} \tag{14}$$

where p is the momentum of the particle. This matches the behavior of a particle in dS.

The time that it takes for the particle to reach distance R from the pode is

$$t_* \approx \log R. \tag{15}$$

I have intentionally used the notation t_*, which is the conventional notation for the scrambling time. The reason for this will shortly become clear.

The inverted oscillator is characterized by an operator algebra, including the Hamiltonian, and, for each direction, a generator $L_\pm$, defined by

$$L_\pm = \frac{x \pm p}{\sqrt{2}}. \tag{16}$$

The algebra, which I will call the *symmetry* of the model, is,

$$\begin{aligned} [H, L_-] &= iL_- \\ [H, L_+] &= -iL_+ \\ [L_-, L_+] &= i. \end{aligned} \tag{17}$$

From the first two relations, it follows that,

$$\begin{aligned} L_-(t) &= L_- e^{-t} \\ L_+(t) &= L_+ e^t \end{aligned} \tag{18}$$

The algebra is satisfied by a generalization to a system of many non-interacting particles, as well as particles coupled by translationally invariant forces.

The toy model, as defined up to this point, is the semiclassical limit of a more complete model, which has a stretched horizon, a finite entropy, and nonperturbative effects.

3.1. Toy Model with Stretched Horizon

To date, in the toy model, the particle has potential for an infinite amount of time before reaching $r = \infty$. This parallels the fact that, classically, a particle takes infinite time to reach the de Sitter horizon.

To make a more interesting model, the radial direction can be cut off by turning the potential sharply upward at a distance R from the pode. Instead of a single particle, we can introduce N particles, which are allowed to interact, but only when they are very near the bottom of the potential. The details of the interaction are not important except that they lead to chaotic behavior and thermalization.

Figure 10 illustrates the setup. The first panel shows the potential, along with N particles in thermal equilibrium at the bottom. The second panel is the view-from-above, in which we see the particles occupying a two-dimensional shell at distance R from the pode. This shell is the toy model version of the stretched horizon.

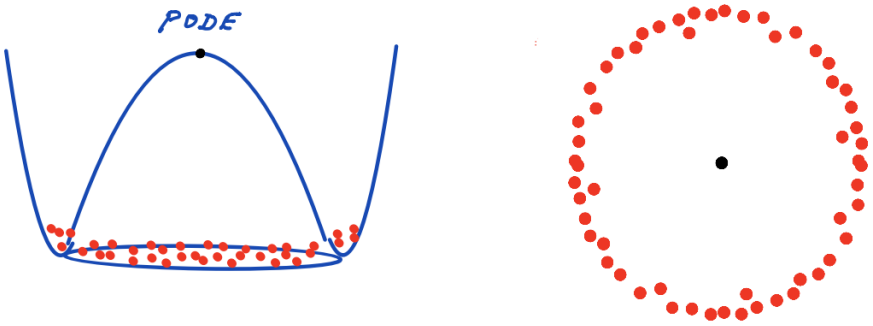

Figure 10. Toy model with stretched horizon. The right panel shows the view from above.

The number of particles can be chosen so that the area-density at the stretched horizon is of the order $1/G$. The entropy of the thermal gas is proportional to the number of particles with an appropriate choice of temperature and other numerical constants,

$$\begin{aligned} S_0 &= \frac{\text{Area}}{4G} \\ &= \frac{\pi R^2}{G} \end{aligned} \tag{19}$$

The time that it takes for a particle to fall from the pode to the stretched horizon is the scrambling time.

The semiclassical limit is identified with the limit $R \to \infty$. With that limit, the entropy becomes infinite and the thermal state is very boring to an observer at the pode. Thermal fluctuations do occur, but the potential well is so deep that the probability of a particle in the equilibrium "soup" reaching the pode is zero.

3.2. Fluctuations

If R (and, therefore, the entropy) is kept finite, there is a non-zero probability of finding one or more particles at the pode. The particles could form interesting objects such as black holes, galaxies, or brains. These nonperturbative Boltzmann fluctuations are extremely rare, but they are the only things that occur in thermal equilibrium [8].

Consider the probability of a Boltzmann fluctuation in which an object $\mathcal{O}$ materializes at the pode. To mathematically represent this situation, we introduce a projection operator $\Pi_{\mathcal{O}}$ that projects onto states in which the object $\mathcal{O}$ is present at the pode. This probability is given by

$$P_{\mathcal{O}} = Tr\ \rho \Pi_{\mathcal{O}} \tag{20}$$

where ρ is the thermal density matrix.

Non-equilibrium dynamics are encoded in the thermal state. For example, suppose we want to know the probability that if the object $\mathcal{O}$ is present at $t = 0$, then, at a later time, t will have made a transition to $\mathcal{O}'$. This is encoded in the correlation function,

$$Tr\rho\ \Pi_{\mathcal{O}}\ e^{-iHt}\ \Pi_{\mathcal{O}'}\ e^{iHt} = Tr\rho\ \Pi_{\mathcal{O}}(0)\ \Pi_{\mathcal{O}'}(t) \tag{21}$$

This type of formula, and its generalizations, show that the theory of fluctuations in thermal equilibrium encodes a very rich spectrum of dynamical phenomena.

The probability $P_{\mathcal{O}}$ is given by a standard expression,

$$P_{\mathcal{O}} = e^{-\Delta S} \tag{22}$$

where the "entropy-deficit" ΔS is defined by,

$$\Delta S = S_0 - S_{\mathcal{O}}. \tag{23}$$

This formula requires some explanation. The symbol S_0 stands for the de Sitter entropy $\pi R^2/G$. $S_{\mathcal{O}}$; however, it does not stand for the entropy of the object $\mathcal{O}$. It is the conditional entropy of the whole system, given that the object $\mathcal{O}$ is present at the pode. A simple way of thinking about $S_{\mathcal{O}}$ is that it represents the entropy of the remaining horizon degrees of freedom, given that $\mathcal{O}$ is present, plus the entropy of $\mathcal{O}$. We will return to this in Section 5.2.

3.3. The GKS Anomaly

Can the algebra (17) be satisfied in the cutoff model? With the identification (16) and modification of the Hamiltonian required to construct the cutoff model, the algebra will not hold, but one may ask if there can be new operators $L_{\pm}$, which, along with the new Hamiltonian, satisfy this. The answer is no [1]. To prove this[11], we consider the first of Equations (18) (a consequence of the algebra) and take its matrix element between normalizable states,

$$\langle \psi | L_-(t) | \psi \rangle \to e^{-t} \to 0. \tag{24}$$

The argument for the GKS anomaly contains two parts:

1. Finiteness of entropy implies that the energy spectrum is discrete. More exactly, it says that the number of states below any given energy is finite. This is much weaker than saying that the Hilbert space is finite-dimensional, which we do not assume.
2. Functions defined as sums of the form,

$$F(t) = \sum_i a_i e^{iE_i t} \tag{25}$$

cannot reach zero as $t \to \infty$. They will have fluctuations and even recurrences over very long timescales. One can easily prove that the late-time variance of $F(t)$ satisfies,

$$\lim_{T\to\infty} \frac{1}{T} \int_0^T |F^2| dt = \sum_i |a_i|^2 > 0 \tag{26}$$

In other words, over long periods of time, F will fluctuate, with a variance equal to $\sum_i |a_i|^2$.

It follows [1] that (24) (and the algebra (17), which led to it) cannot be satisfied if the entropy is finite. There is a deep relationship between fluctuations and the non-perturbative breaking of semiclassical symmetries.

We can be more quantitative. In the semiclassical limit, the energy spectrum is continuous, and (25) is replaced by,

$$F(t) = \int A(E) e^{iEt}. \tag{27}$$

If $A(E)$ is square integrable, then $F(t) \to 0$ as $t \to \infty$. In approximating the sum by an integral, we make the following correspondence:

$$a_i = A(E)\delta E \tag{28}$$

where δE is the spacing between neighboring energy levels. Now, consider the sum in (26) and rewrite it in terms of A.

$$\begin{aligned} \sum |a_i|^2 &= \sum |A(E)|^2 (\delta E)^2 \\ &\to \int |A(E)|^2 \delta E dE \end{aligned} \tag{29}$$

The energy level spacings δE are of order e^{-S_0}. Thus it follows that $|\sum a_i|^2 \sim \delta E \sim e^{-S_0}$, and from (26),

$$\mathrm{Var}(L_-) \sim e^{-S_0}. \tag{30}$$

Given that the symmetry algebra requires asymptotic variance in L_- to be zero, the actual variance in (30) is a measure of how badly the symmetry is broken by the anomaly.

More generally, it seems reasonable to suppose that the discreteness of the energy spectrum produces effects that scale as a power of e^{-S_0}.

The bottom line is that fluctuations of the order e^{-S_0} create an obstruction to realizing the symmetry algebra (17) as long as the entropy is finite.

3.4. Caveats

The toy model has elements in common with de Sitter space; however, like all analogies, it has limitations. Two come to mind: First, because it is based on non-relativistic particles, it cannot capture the physics of massless photons in de Sitter space. For example, the probability of finding a single thermal photon of wavelength $\sim R/2$ within a distance $\sim R/2$ of the pode is in the order of 1. This is a perturbative phenomenon, which would requires massless relativistic degrees of freedom instead of massive non-relativistic particles.

Another unphysical feature of the toy model is that the size of the horizon is fixed, while the size of the de Sitter horizon is dynamic and can adjust to the amount of entropy that it contains (see Section 5.2).

4. The GKS Anomaly in JT/SYK

A similar anomaly to that seen in Section 3.3 also affects two-dimensional models such as JT gravity, and its quantum SYK completion. Figure 11 shows the $AdS(2)$ solution of JT gravity with Rindler-like horizons.

The classical theory[12] has an exact $SL(2R)$ symmetry, which persists for all orders in perturbation theory; in other words, it is a feature of the semiclassical theory. However, the symmetry is broken by non-perturbative quantum effects [13]. The $SL(2R)$ group has three generators, $\mathcal{T}$, H and $\mathcal{P}$, whose action is illustrated diagramatically [14] in the three panels of Figure 11.

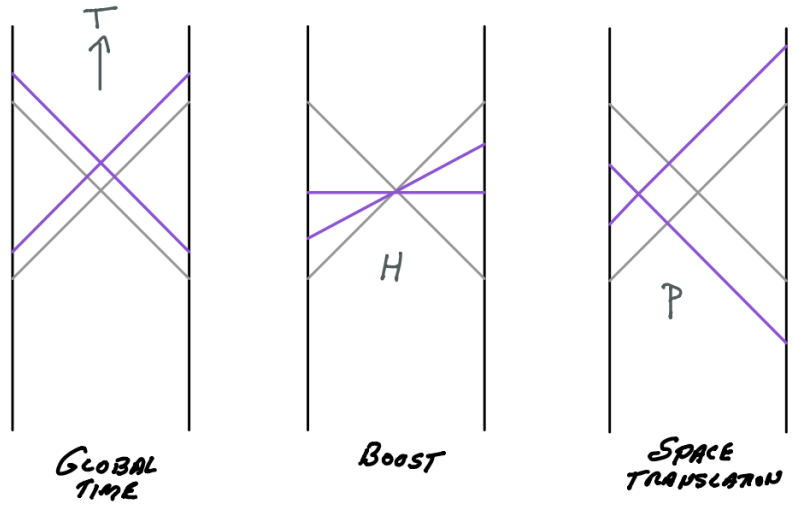

Figure 11. The three generators of $SL(2R)$: $\mathcal{T}$ generates global time translations and vertically shifts the horizon; H is the boost Hamiltonian that generates Rindler-like boosts; and $\mathcal{P}$ generates space-like shifts in the horizon. Only H does not move the horizon.

The generator $\mathcal{T}$ generates global time shifts and moves the horizons vertically from their original location (grey lines) to a new location (purple lines.) The generator H is the boost Hamiltonian that holds the horizons fixed but acts on equal-time-slices to boost them. Finally, $\mathcal{P}$ generates a spacelike displacement of the horizon, as shown. $\mathcal{T}$ and $\mathcal{P}$ are analogous to the hard generators of $O(d,1)$, and H is easy.

These generators satisfy the $SL(2R)$ algebra,

$$\begin{aligned}[H,\mathcal{T}] &= i\mathcal{P}\\ [H,\mathcal{P}] &= i\mathcal{T}\\ [\mathcal{T},\mathcal{P}] &= iH\end{aligned} \tag{31}$$

which is semiclassically exact, but cannot hold non-perturbatively. To show this, we define the light-like generators,

$$\begin{aligned}L_- &= \frac{\mathcal{P}-\mathcal{T}}{\sqrt{2}}\\ L_+ &= \frac{\mathcal{P}+\mathcal{T}}{\sqrt{2}}.\end{aligned} \tag{32}$$

From (31),

$$i[H,L_\pm] = \pm L_\pm \tag{33}$$

implying,

$$L_\pm(t) = L_\pm e^{\pm t}. \tag{34}$$

In the classical JT system, the entropy is infinite and Equation (34) presents no problem, but in a quantum completion such as SYK, the entropy is finite, of the order of the number of fermion species N. The rest of the argument is identical to the one in Section 3.3 and implies that the $SL(2R)$ symmetry cannot be exact, except in the limit $N \to \infty$.

All of this is well-known from other perspectives [13,14], and it is believed that the breaking of the symmetry can be understood in terms of higher genus corrections to the integral JT path.

5. de Sitter

Returning to the de Sitter space and static patch holography, insofar as the static patch is in thermal equilibrium with finite entropy, it will undergo Boltzmann fluctuations. As we saw in Section 3.3, these fluctuations are the source of the symmetry-breaking in the toy model. This section will discuss the anomaly in the $O(d,1)$ de Sitter symmetry and explain how general relativity can be used to provide a quantitative account of Boltzmann fluctuations

5.1. The O(d,1) Anomaly

Now, let us return to the symmetry algebra of de Sitter space. From the last two of Equations (3), we may construct light-like generators,

$$L_\pm = \frac{\mathcal{J}_2 \pm \mathcal{K}_1}{\sqrt{2}} \tag{35}$$

satisfying,

$$i[H,L_\pm] = \pm L_\pm. \tag{36}$$

Note that these equations are identical to the first two equations in (17) and that they imply,

$$L_-(t) = L_-(0)e^{-t}. \tag{37}$$

Following the same logic as in Section 3.3, we may evaluate this equation between normalizable states to find,

$$\langle\psi|L_-(t)|\psi\rangle \to 0. \tag{38}$$

For the same reasons, as in Section 3.3 and in [1] (relating to persistent fluctuations), there is a GKS anomaly, making it impossible to satisfy (38), and, therefore, the algebra.

The arguments of Section 3.3 concerning fluctuations provide the same estimate for the magnitude of the anomaly effects,

$$\mathrm{Var}(L_-) \sim e^{-S_0}. \tag{39}$$

5.2. Using GR to Calculate Fluctuation Probabilities

In theories with a gravitational dual, general relativity provides a precise way of calculating the probability of certain fluctuations. Consider the rate for fluctuations that nucleate massive objects, such as black holes near the pode. We can use (22) and (23) to compute the rate. To calculate S_0, we can use the metric (1) to obtain the radius of the horizon (we get $r_H = R$), then calculate the area of the horizon, and, finally, the entropy. The result is

$$S_0 = \frac{\pi R^2}{G}. \tag{40}$$

Next, consider the metric of de Sitter space with an object $\mathcal{O}$ of mass M at the pode. The effect of the mass is to pull in the cosmic horizon, shrinking its area and, therefore, its entropy [15–17]. Beyond the radius of the object, the metric takes the form (1), except that the emblackening factor $f(r)$ is replaced by

$$f_M(r) = \left(1 - \frac{r^2}{R^2} - \frac{2MG}{r}\right). \tag{41}$$

The horizon location is defined by $f_M(r) = 0$. Multiplying by r, this becomes,

$$r - \frac{r^3}{R^2} - 2MG = 0 \tag{42}$$

Equation (42) has three solutions, two with positive r and one with negative r. The negative solution is unphysical. The larger of the two positive solutions determines the location of the cosmic horizon and the smaller determines the horizon of a black hole of mass M. At the lowest order in M, the cosmic horizon is shifted to a new value of r, given by,

$$r = R - MG \tag{43}$$

The entropy is given by

$$S_{\mathcal{O}} = \frac{\pi(R - MG)^2}{G} \tag{44}$$

and (to the leading order in M) the entropy-deficit is given by [15],

$$\Delta S = 2\pi MR. \tag{45}$$

Now, recall that the inverse temperature of de Sitter spaceis $\beta = 2\pi R$. Using (22), we find

$$P_{\mathcal{O}} = e^{-\beta M}. \tag{46}$$

Equation (46) is the Boltzman weight for a configuration of energy M. The answer itself is not surprising but what is interesting is that the connection between entropy and area has been used in a new way—not for equilibrium probabilities, but for fluctuations away from average behavior.

More generally, we can move beyond linear order in M. Let us denote the two solutions of (42) by r_- and r_+ and define the independent parameter,

$$x = (r_+ - r_-). \tag{47}$$

One can express x in terms of the mass of the black hole by eliminating r_+ and r_- from the equations,

$$\begin{aligned} R^2 &= r_+^2 + r_-^2 + r_+ r_- \\ 2MGR^2 &= r_+ r_- (r_+ + r_-) \\ x &= r_+ - r_- \end{aligned} \tag{48}$$

The value of x runs from $(x = -R)$ to $(x = +R)$. Changing the sign of x interchanges the cosmic and black hole horizons. It is convenient to think of positive and negative values of x as different configurations; for example, at both $x = -R$ and $x = +R$, there is a vanishingly small horizon and a maximally large horizon, but we regard these two states as different.

The entropy and entropy-deficit are given by

$$\begin{aligned} S_{\mathcal{O}} &= \frac{\pi}{G}\left(r_+^2 + r_-^2\right) \\ \Delta S &= \frac{\pi}{G}\left(R^2 - r_+^2 - r_-^2\right) \end{aligned} \tag{49}$$

Let us consider the "Nariai point" $(x = 0)$ at which $(r_+ = r_-)$. One can easily find that, at the Nariai point,

$$\begin{aligned} r+^2 &= r_-^2 \\ &\equiv r_N^2 \\ &= \frac{R^2}{3} \end{aligned} \tag{50}$$

From (49) and (50), we find

$$\begin{aligned} S_N &= \frac{2S_0}{3} \\ \Delta S_N &= \frac{S_0}{3} \end{aligned} \tag{51}$$

It is not obvious that ΔS is smooth at $x = 0$. One might expect that $\Delta S(x)$ has a cusp, as in the top panel of Figure 12. However, explicit calculations show that the dependence is completely smooth and surprisingly simple,

$$\Delta S = \frac{S_0}{3}\left(1 - \frac{x^2}{R^2}\right). \tag{52}$$

This is illustrated in the bottom panel of Figure 12.

The total probability of a black hole fluctuation is given by an integral[13] over x,

$$\begin{aligned} \text{Prob} &= \frac{1}{R^4}\int_0^R e^{-\Delta S} x^3 dx \\ &= e^{\frac{-S_0}{3}}\frac{1}{R^4}\int_0^R e^{\frac{S_0 x^2}{3R^2}} x^3 dx. \end{aligned} \tag{53}$$

One finds,

$$\text{Prob} \sim \frac{3G}{\beta R^2}\left(1 + \frac{3}{S_0}e^{-S_0/3}\right) \tag{54}$$

The first term in (54) comes from the endpoint of the integration at $x^2 = R^2$ and is perturbative in G. It is associated with the lightest black holes and numerically dominates the integral. The second term comes from the saddle point at $x = 0$. It can be re-written as

$$e^{-\frac{\pi R^2}{3}\frac{1}{G}}.$$

This is obviously non-perturbative in G. We will discuss its meaning in the next section.

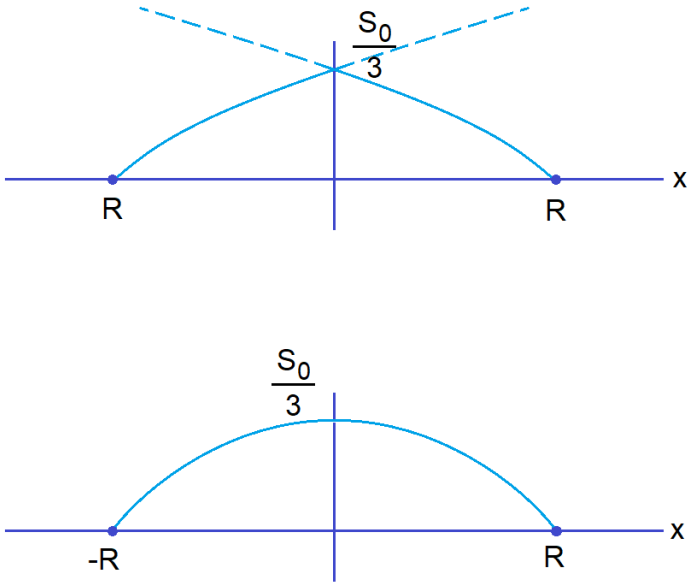

Figure 12. Entropy deficit and a function of x. The upper panel incorrectly shows a cusp at the Nariai point. The lower panel shows the correct smooth behavior (52).

6. The Nariai Geometry

Quantum-mechanically, the non-perturbative fluctuations we are discussing originate from the discreteness of the energy spectrum. On the gravitational side, those same effects are encoded in higher-genus[14] contributions to the gravitational (Euclidean) path integral [18–22]. In the case of anti-de-Sitter space, the contributing geometries are constrained to have asymptotic AdS-like boundary conditions, but subject to that constraint they can have any topology. In the case of Euclidean de Sitter space, there are no boundaries; the path integral, therefore, includes all closed topologies. Among these are the Nariai geometries.

To illustrate the connection between fluctuations and higher-genus contributions, consider the fluctuations discussed in Section 5.2, in which a black hole is spontaneously created near the pode. The first panel of Figure 13 shows the Penrose diagram for a Schwarzschild- de Sitter black hole. A slice through the time-symmetric space-like $t = 0$ surface is depicted in green. In the lower panel, the geometry of such a slice is shown for two different masses of the black hole. The figure on the right depicts a relatively larger mass than that on the left.

One may continue the $t = 0$ geometry in either Minkowski or Euclidean signature. The Minkowski continuation returns the geometry in the top panel of Figure 13. The Euclidean continuation has a compact geometry with the topology $S_2 \times S_2$, which I call an S-geometry (Euclidean Schwarzschild de Sitter). There is a one-parameter family of S-geometries, parameterized by the mass M of the black hole.

The metric of the S-geometry is

$$ds^2 = \left(1 - \frac{r^2}{R^2} - \frac{2MG}{r}\right)d\tau^2 + \left(1 - \frac{r^2}{R^2} - \frac{2MG}{r}\right)^{-1} dr^2 + r^2 d\Omega^2 \tag{55}$$

The one thing left to specify is the range of the periodic Euclidean time τ. Normally, the periodic constraint requires $0 < \tau \leq \beta$, where β signifies inverse temperature. However, in the present case, there is no well-defined temperature because the black hole and cosmic horizon have very different temperatures. For a small black hole, β is $4\pi MG$, while the de Sitter value of β is $2\pi R$. The black hole is out of equilibrium with the de Sitter space.

What this means is that it is not geometrically possible to avoid a conical singularity at either the black hole or the cosmic horizon. For this reason, the S spaces are not genuine saddle points of the Euclidean gravitational path integral—with one exception. The exception is the Nariai space, i.e., S-space at the symmetric point $x = 0$. The geometry of Nariai space is $S_2 \times S_2$ and its Minkowski continuation is $S_2 \times dS_2$, i.e., a spatial sphere times two-dimensional de Sitter space.

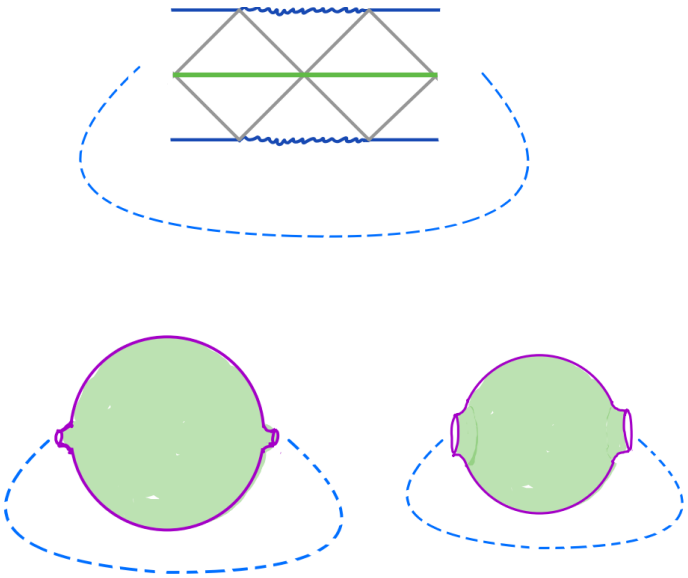

Figure 13. De Sitter-Schwarzschild black hole. The upper panel shows the Penrose diagram and the two lower panels show the spatial geometry of time-symmetric slices. In each case, the dashed blue curves indicate geometric identifications.

Nariai space is a genuine Euclidean saddle point whose Minkowski continuation is often called the Nariai black hole. To understand this better, return to the S-space with a small black hole. A static patch is also shown in the upper panel of Figure 14. As the black hole is at the center of the static patch, we cannot think of the pode as a point. Instead, I have indicated a shell with a dashed red line. The shell is a two-sphere that surrounds the black hole between the black hole horizon (black dot) and the cosmic horizon (purple dot).

A spatial $t = 0$ slice of the geometry between the two horizons is shown in the lower panel.

Now, let us consider deforming the geometry by increasing the black hole mass and, at the same time, decreasing the cosmic horizon area (following the curve in the lower panel of Figure 12) until we reach the Nariai point. At that point, the geometry—not just the topology— is $S_2 \times S_2$, but from the viewpoint of the static patch observer, it looks like a spatial interval times a 2-sphere. The observer is sandwiched between two equal horizons.

Thought of as a real process, this history would violate the second law of thermodynamics, but as long as S_0 is finite, it can occur as a rare Boltzmann fluctuation. It requires energy to be transferred from the cosmic horizon to the black hole—a kind of anti-evaporation. The most likely trajectory of this system is the time reverse of the evaporation process, in which one of the two Nariai horizons spontaneously emits radiation, which is then absorbed by the other. When this happens, the emitter loses energy and becomes hotter. The result is that it emits more energy until the smaller horizon becomes a small black hole (or even no black hole) and the larger horizon reaches entropy S_0. The

time-reverse of this process is the Boltzmann fluctuation, which leads to the Nariai state from the small black hole state.

Once the Nariai state is achieved, it is unstable. One possibility is that the system can return to the original state, with the original black hole shrinking and the original cosmic horizon returning to its full dS size. However, the opposite can also occur: the system overshoots and the original black hole keeps absorbing energy while the original cosmic horizon shrinks to a small black hole. We can think of this as a transition from from $x = -R$ to $x = +R$. An observer between the two horizons sees a surprising history, in which the geometry of the static patch turns itself "inside-out"—the outer cosmic horizon and the inner black hole horizon exchange roles. This remarkably strange event is illustrated in Figure 15.

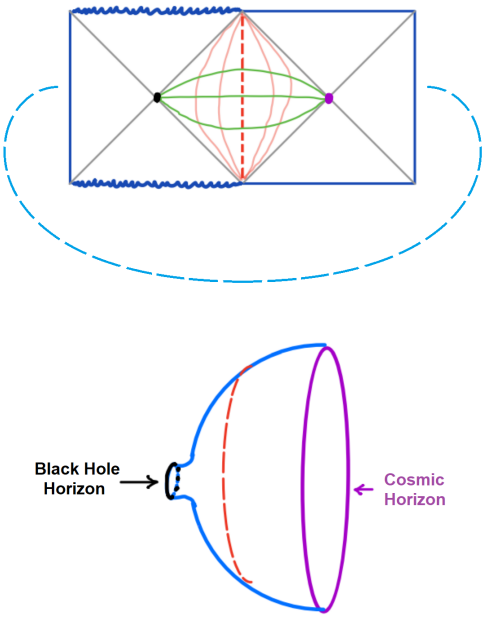

Figure 14. The top panel shows the penrose diagram for a Euclidean Schwarzschild black hole, together with a static patch, which symmetrically encloses the black hole. The black dot on the left is the black hole horizon. The purple dot on the right is the cosmic horizon. The lower panel shows a spatial slice of the region between the two horizons. The dashed red line indicates the static position of a 2-sphere somewhere between the two horizons.

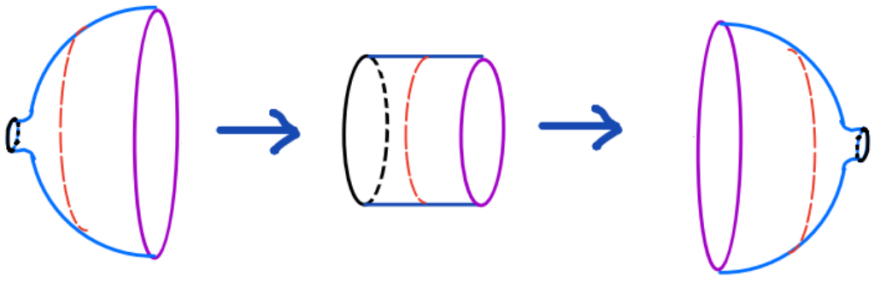

Figure 15. The "inside-out transition" in which a small black hole horizon and the cosmic horizon interchange by passing through the intermediate Nariai black hole.

6.1. Nariai and Hawking-Moss

One might be tempted to think of this inside-out transition as a quantum tunneling event, but, unlike a typical quantum tunneling, the process stretches out over a long time. The energy transfer is simply Hawking evaporation or its time-reverse, and takes the same order as the Page time[15]. The transition is a thermal process, mediated by a Hawking–Moss instanton [23], not a quantum tunneling event. It takes a very long time, during which the

system sits at or near the top of the potential, i.e, at $x = 0$. The Hawking–Moss instanton calculates the probability that the system in question is at the top of a broad potential barrier [24].

In this case, the Hawking–Moss instanton is the Nariai geometry, $S_2 \times S_2$ and the probability of finding the system in the Nariai state is

$$e^{-\Delta I_N},$$

where I is the action-deficit of Euclidean Nariai space. Not surprisingly, that action deficit is the same as the entropy-deficit of the Nariai black hole,

$$\Delta I_N = \frac{S_0}{3}. \tag{56}$$

Thus, we see an example of the relationship between fluctuations (the appearance of a Nariai black hole) and a higher genus wormhole geometry (the $S_2 \times S_2$ Nariai geometry.)

6.2. Connection with Anomaly

What does all of this have to do with the $O(d, 1)$ symmetry (or lack of it) in de Sitter space? I think the answer is fairly simple. In the Euclidean continuation, the symmetry group is $O(5)$. There is a natural action of the $O(5)$ group on the semiclassical Euclidean dS geometry, namely, S_4. However, the full path integral receives contributions from other topologies, particularly the Nariai geometry $S_2 \times S_2$. Trying to define the action of $O(5)$ on $S_2 \times S_2$ is like trying to define the action of $O(3)$ on a torus. It is not that the torus breaks the symmetry like a egg would; the symmetry operations just do not exist on the torus. Likewise, the generators of $O(5)$ do not exist on $S_2 \times S_2$.

One might try to get around this by defining the action of the group as trivial on all higher topologies; in other words, define $S_2 \times S_2$ as invariant under $O(5)$. I think the reason that this does not work is that, in general, different topology states are not orthogonal: the overlaps are of the order $\exp(-S)$ [21]. For this reason, the action of the group on $S_2 \times S_2$ cannot be arbitrarily chosen, independently of the action on S_4.

Thus, we are left with the conclusion that higher topologies not only break the symmetry of dS: they do not even allow for it to be defined. This is consistent with the GKS anomaly, which also implies that the generators cannot consistently be constructed to order $\exp(-S_0)$.

7. Implications of the Anomaly

The group $O(d, 1)$ relates different static patches within a single de Sitter space. For example, in Figure 16 shows two static patches, which are related by the action of a light-like generator L.

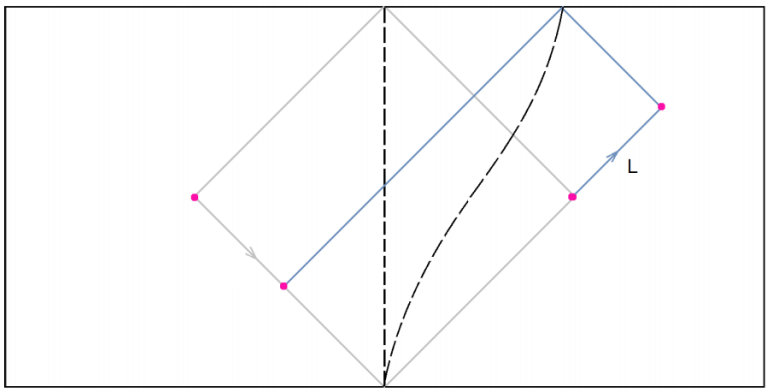

Figure 16. Two-dimensional de Sitter spacewith two static patches related by a light-like generator L.

If the $O(d,1)$ symmetry is not broken by the GKS, anomaly one would expect that the dynamics in the two patches would be identical. In particular, the Hamiltonian in one patch would be related to that in the other patch by a unitary transformation and the two spectra would be identical. However, our result suggests that this is not true; it is likely is that the coarse-grained spectra of the two Hamiltonians are the same but, at the discrete level of individual eigenvalues, the spectra do not match. The occurrence and timing of fluctuations in the two static patches (for example, quantum recurrences) would be different. The Hamiltonians for different patches might be drawn from a single ensemble, but would be different instances of that ensemble. In the absence of knowledge about which Hamiltonian governs an observer's patch, averaging over the ensemble would make sense[16].

Gauge Symmetry?

It is usually assumed that the $O(d,1)$ relating different static patches is a gauge symmetry, or a redundancy of the description. However, having a gauge symmetry requires that the gauge transformation can be consistently defined. This does not appear to be possible for the symmetries of de Sitter space except in the semiclassical limit. The GKS anomaly precludes the existence of the generators to a higher order in e^{-S_0} and indicates that different static patches are inequivalent when effects of the order e^{-S_0} are considered. Thus, the answer to this question is that $O(d,1)$ should be treated as a gauge symmetry in the semiclassical approximation, but not in the full, non-perturbative theory. One could select a static patch not by gauge fixing, but by simply selecting the patch whose detailed energy levels have some specific pattern.

One possible conclusion is that eternal de Sitter space is not consistent—a view taken in [1]. In this paper, I have advocated for another viewpoint; namely, that the de Sitter symmetries are approximate, and valid in classical theory and in perturbation theory, but not beyond. In fact, for other topologies, the action of $O(d,1)$ may not even be defined. For example, it is hard to imagine the action of $O(d,1)$ on the Nariai space $S(2) \times S(2)$.

In some ways, the situation seems similar to recent discussions of global symmetries and their breaking by higher topologies [27], where it was suggested that global symmetries (forbidden by gravity) may be restored in the ensemble average. In the context of de Sitter space, the average over all the static patches in de Sitter spacemight have the symmetry that the individual instances lack.

8. Conclusions

Eternal de Sitter space is a space–time without time-like boundaries, but a static patch is bounded by a horizon. On the basis of covariant entropy bounds, I argued that the natural place to locate holographic degrees of freedom is on the stretched horizon. The only things that happen in eternal de Sitter space are fluctuations in these horizon degrees of freedom, which, from the bulk perspective, sporadically produce interesting objects deep in the interior of the static patch.

We have explored three non-perturbative de Sitter space phenomena related to these fluctuations. The first was the violation of the de Sitter symmetry $O(4,1)$ due to the GKS anomaly. The variance $\mathrm{Var}(L_-)$ in (39) is a measure of the magnitude of the violation.

The second was large-scale Boltzmann fluctuations, in which the holographic horizon degrees of freedom undergo freak rearrangements, leading to large black holes materializing in the interior of the static patch. The probability of this happening is given by (54). The second term of this expression is non-perturbative and represents the creation of the largest black holes with entropy $\approx S_0/3$.

Finally, wormholes and higher genus geometries, a saddle point due to the Nariai geometry $S_2 \times S_2$, non-perturbatively contribute to the gravitational path integral and describe a massive fluctuation, in which de Sitter space turns itself "inside out".

These phenomena, which all scale exponentially with $-S_0$, are closely connected. One might even say they express the same underlying fact; namely, the discreteness of

the energy spectrum, and finite-level spacing $\delta E \sim e^{-S}$. Moreover, they are extensions of things that have been observed in other contexts such as SYK and JT gravity; the novelty is that they appear in the holography of de Sitter space.

The violation of symmetry is especially interesting. This means that different static patches are inequivalent. They may have different Hamiltonians and different energy spectra, but the coarse-grained spectra must be the same to ensure a universal semiclassical limit. Although this is an open question, it is interesting to conjecture that the symmetry-violation is washed out by some form of ensemble averaging, as is thought to be the case for JT gravity.

Funding: This research received no external funding.

Acknowledgments: I am grateful to Adel Rahman, and Douglas Stanford for discussions, and especially to Adam Brown for discussions about the Nariai saddle point.

Conflicts of Interest: The authors declare no conflict of interest.

Notes

1 By cold, I mean non-fluctuating. By warm, I mean the opposite.

2 The framework for [1] was the same as for this paper; namely, it assumed that a static patch of de Sitter space has a holographic description based on conventional Hamiltonian quantum mechanics.

3 The notation exp will be used to indicate a general exponential scaling. Thus, e^S, $e^{S/3,}$ and e^{2S} are all exp (S).

4 From the perspective of a static patch.

5 Strictly speaking, a true Penrose diagram would only contain a single square with each point on the diagram representing a zero-sphere, i.e., two points.

6 A "point" on the asymptotic boundary does not literally mean a point, but rather a region of proper size no bigger than R. This is familiar in AdS/CFT where a point on the boundary has N^2 degrees of freedom and represents a region of AdS size [9].

7 Bousso supplements, consider a Penrose diagram with a system of wedge-like symbols showing the direction in which light sheets focus and de-focus.

8 I will use the terms *higher genus* and *wormhole* rather loosely, to mean any connected geometry with a different topology to the original semiclassical geometry. For Euclidean dS, the semiclassical geometry has four spheres. Any other connected topology is, by definition, a higher-genus wormhole.

9 See Section 7.

10 With the normalization of the Hamiltonian defined by (3), the temperature of the static patch has the value $T = 1/2\pi$.

11 A more rigorous version of the proof was given in [1].

12 JT gravity coupled to matter, with the matter being uncoupled to the dilaton. I am grateful to Douglas Stanford and Henry Lin for explaining this to me.

13 The factor x^3 in the integrand of (53) is due to three negative modes associated with the instability of an object located at the pode. See Figure 9 and Equation (12).

14 See footnote 3 in Section 2.4.

15 One should distinguish two time scales. The first is how long the inside-out transition takes. This is the same order as Page time. The second is the typical time between such events. This latter time scale is exponential $\sim e^{S_0/3}$.

16 Similar ideas have long been advocated by Banks and Fischler [25,26], who argue that many static-patch Hamiltonians may lead to identical observations. Their argument is quite different from the one in this paper. It is based on assumed limits of observation in a closed world with finite entropy.

References

1. Goheer, N.; Kleban, M.; Susskind, L. The Trouble with de Sitter space. *J. High Energy Phys.* **2003**, *7*, 56. [CrossRef]
2. Bousso, R.; Freivogel, B.; Yang, I.S. Eternal Inflation: The Inside Story. *Phys. Rev. D* **2006**, *74*, 103516. [CrossRef]
3. Harlow, D.; Shenker, S.H.; Stanford, D.; Susskind, L. Tree-like structure of eternal inflation: A solvable model. *Phys. Rev. D* **2012**, *85*, 063516. [CrossRef]
4. Susskind, L. Fractal-Flows and Time's Arrow. *arXiv* **2012**, arXiv:1203.6440.
5. Susskind, L. Was There a Beginning? *arXiv* **2012**, arXiv:1204.5385.
6. Susskind, L. Is Eternal Inflation Past-Eternal? And What if It Is? *arXiv* **2012**, arXiv:1205.0589.
7. Dyson, L.; Lindesay, J.; Susskind, L. Is there really a de Sitter/CFT duality? *J. High Energy Phys.* **2002**, *8*, 45. [CrossRef]
8. Dyson, L.; Kleban, M.; Susskind, L. Disturbing implications of a cosmological constant. *J. High Energy Phys.* **2002**, *10*, 11. [CrossRef]

9. Susskind, L.; Witten, E. The Holographic bound in anti-de Sitter space. *arXiv* **1998**, arXiv:hep-th/9805114.
10. Maldacena, J.M. Eternal black holes in anti-de Sitter. *J. High Energy Phys.* **2003**, *4*, 21. [CrossRef]
11. Bousso, R. A Covariant entropy conjecture. *J. High Energy Phys.* **1999**, *7*, 4. [CrossRef]
12. Fischler, W.; Susskind, L. Holography and cosmology. *arXiv* **1998**, arXiv:hep-th/9806039.
13. Maldacena, J.; Stanford, D.; Yang, Z. Conformal symmetry and its breaking in two dimensional Nearly Anti-de-Sitter space. *Prog. Theor. Exp. Phys.* **2016**, *2016*, 12C104. [CrossRef]
14. Lin, H.W.; Maldacena, J.; Zhao, Y. Symmetries Near the Horizon. *J. High Energy Phys.* **2019**, *8*, 49. [CrossRef]
15. Banks, T.; Fiol, B.; Morisse, A. Towards a quantum theory of de Sitter space. *J. High Energy Phys.* **2006**, *12*, 4. [CrossRef]
16. Susskind, L. Addendum to Fast Scramblers. *arXiv* **2011**, arXiv:1101.6048.
17. Banks, T.; Fischler, W. Holographic Space-time, Newton's Law and the Dynamics of Black Holes. *arXiv* **2016**, arXiv:1606.01267.
18. Cotler, J.S.; Gur-Ari, G.; Hanada, M.; Polchinski, J.; Saad, P.; Shenker, S.H.; Stanford, D.; Streicher, A.; Tezuka, M. Black Holes and Random Matrices. *J. High Energy Phys.* **2017**, *5*, 118; erratum in **2018**, *9*, 2. [CrossRef]
19. Saad, P.; Shenker, S.H.; Stanford, D. A semiclassical ramp in SYK and in gravity. *arXiv* **2018**, arXiv:1806.06840.
20. Saad, P. Black Holes, Baby Universes, and Random Matrices. Ph.D. Thesis, Stanford University, Stanford, CA, USA, 2020.
21. Marolf, D.; Maxfield, H. Transcending the ensemble: Baby universes, spacetime wormholes, and the order and disorder of black hole information. *J. High Energy Phys.* **2020**, *8*, 44. [CrossRef]
22. Almheiri, A.; Mahajan, R.; Maldacena, J.; Zhao, Y. The Page curve of Hawking radiation from semiclassical geometry. *J. High Energy Phys.* **2020**, *3*, 149. [CrossRef]
23. Hawking, S.W.; Moss, I.G. Supercooled Phase Transitions in the Very Early Universe. *Phys. Lett. B* **1982**, *110*, 35–38. [CrossRef]
24. Weinberg, E.J. Hawking-Moss bounces and vacuum decay rates. *Phys. Rev. Lett.* **2007**, *98*, 251303. [CrossRef] [PubMed]
25. Banks, T.; Fischler, W.; Paban, S. Recurrent nightmares? Measurement theory in de Sitter space. *J. High Energy Phys.* **2002**, *12*, 62. [CrossRef]
26. Banks, T. Some thoughts on the quantum theory of de sitter space. *arXiv* **2003**, arXiv:astro-ph/0305037.
27. Chen, Y.; Lin, H.W. Signatures of global symmetry violation in relative entropies and replica wormholes. *J. High Energy Phys.* **2021**, *3*, 40. [CrossRef]